ZIF-8 Metal−Organic Framework Electrochemical Biosensor for the Detection of Protein−Protein Interaction

Luciana D. Trino[¥]; Luiz G. S. Albano[‡]; Daniela C. Granato[¥]; Aline G. Santana[¥,£]; Davi H. S. de Camargo[‡]; Catia C. Correa[‡]; Carlos C. Bof Bufon[‡,€,‼]*; Adriana F. Paes Leme[¥]*

[¥] Laboratório Nacional de Biociências (LNBio), Centro Nacional de Pesquisa em Energia e Materiais (CNPEM), Campinas, São Paulo, 13083-100, Brazil

[‡] Laboratório Nacional de Nanotecnologia (LNNano), Centro Nacional de Pesquisa em Energia e Materiais (CNPEM), Campinas, São Paulo, 13083-100, Brazil

[£] Departamento de Biologia Molecular e Funcional, Instituto de Biologia (IB), Universidade de Campinas (UNICAMP), Campinas, São Paulo, 13083-865, Brazil

[€] Departamento de Físico-Química, Instituto de Química (IQ), Universidade de Campinas (UNICAMP), Campinas, São Paulo, 13083-970, Brazil

[‼] Programa de Pós-Graduação em Ciência e Tecnologia de Materiais (POSMAT), Universidade Estadual Paulista (UNESP), Bauru, São Paulo, 17033-360, Brazil

*Corresponding Authors:
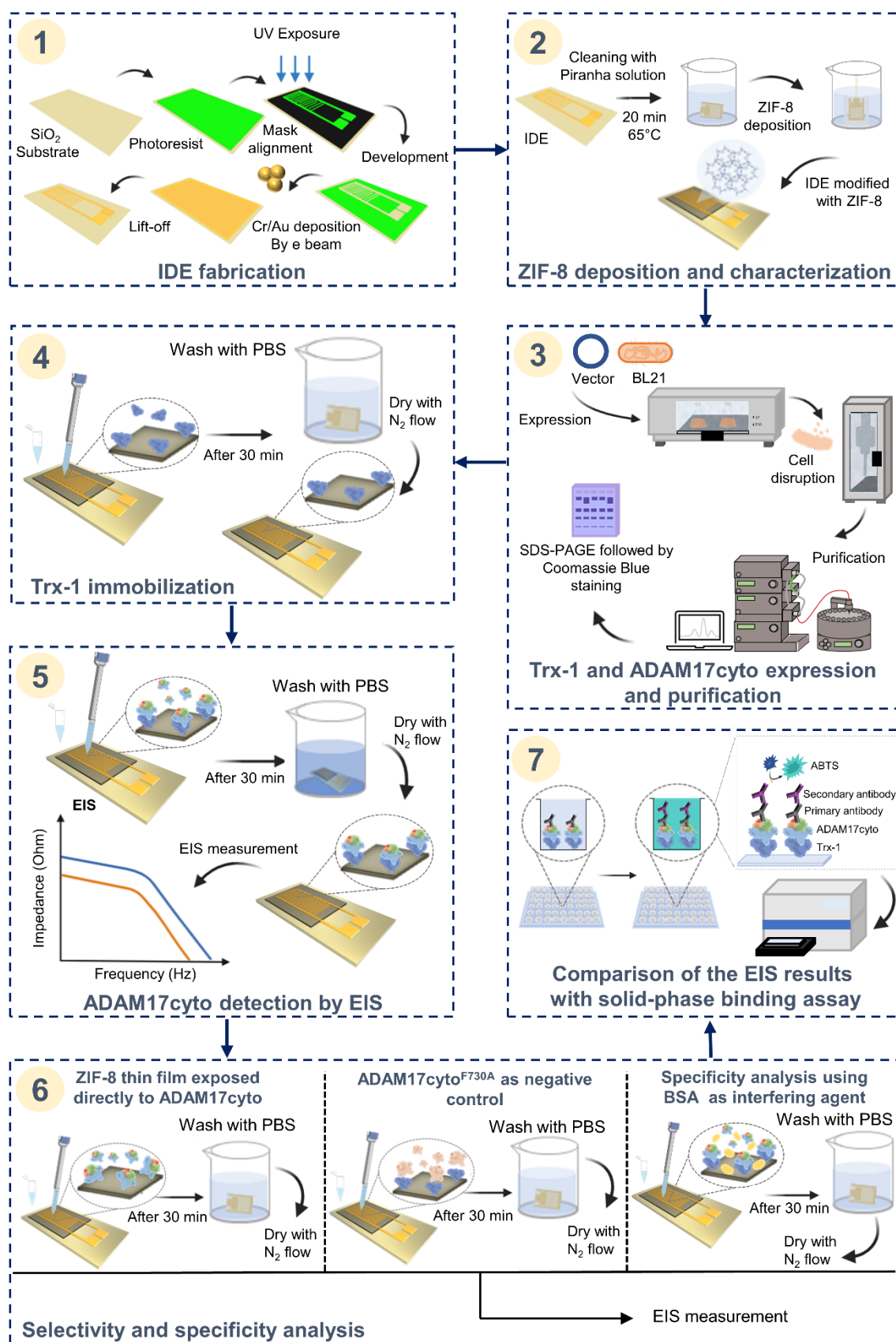adriana.paesleme@lnbio.cnpem.br;
carlos.bufon@lnnano.cnpem.br

Figure S1: Schematic representation of the workflow for the IDE ZIF-8 electrochemical

biosensor development. The first step shows the IDE fabrication using conventional

photolithography. After that, in the second step, the IDE surface was modified with ZIF-8 by immersion in the precursor's solution. Then, the proteins Trx-1 and ADAM17cyto were expressed in BL21 competent cells and purified through affinity and gel filtration chromatography, as shown in step 3. The Trx-1 purified protein was immobilized on the IDE ZIF-8 surface for the latter recognition of ADAM17cyto protein, step 4. The detection of ADAM17cyto in different concentrations (50 nM to 8 µM) by EIS measurements was performed as described in step 5. The biosensor selectivity and specificity analysis were performed in step 6. Finally, the EIS results were compared with the solid-phase binding assay in step 7.
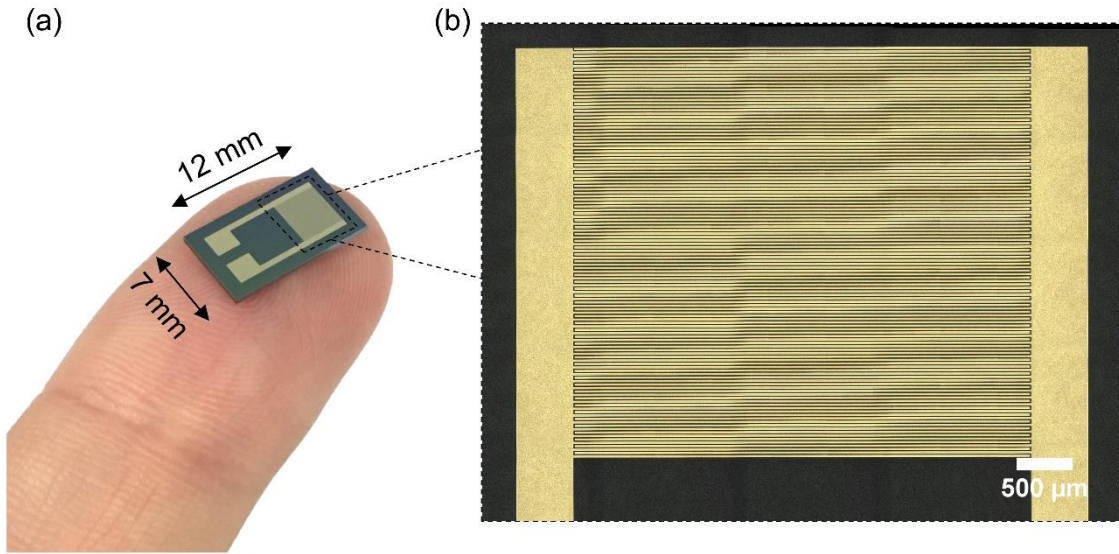
Figure S2: The IDE was fabricated through conventional photolithography; the size of each substrate is shown in (a). (b) Laser scanning confocal microscopy image showing the active area of IDE. The IDEs have 60 electrode arrays confined to a small active area of ~15 mm^2. The distance between each electrode array is 10 µm (channel length) and the total channel width-length (W/L) ratio is 50,000.
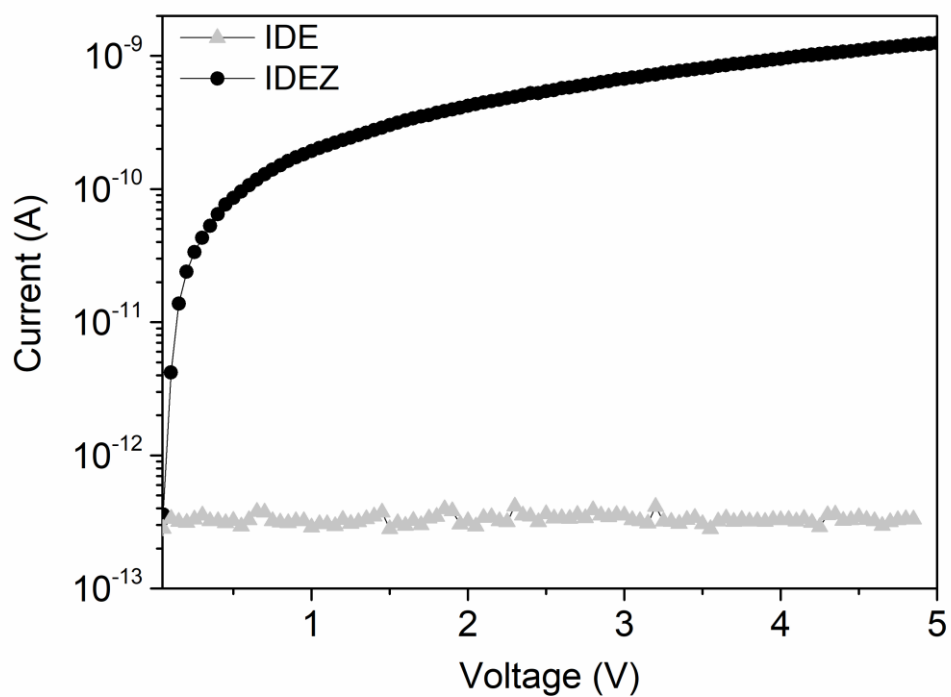
Figure S3: Typical current-voltage curves for IDE before and after ZIF-8 deposition. All IDEs were tested before ZIF-8 deposition to verify the leakage current. The curves show that the electrical current for the empty IDE is lower when compared with IDE ZIF-8.
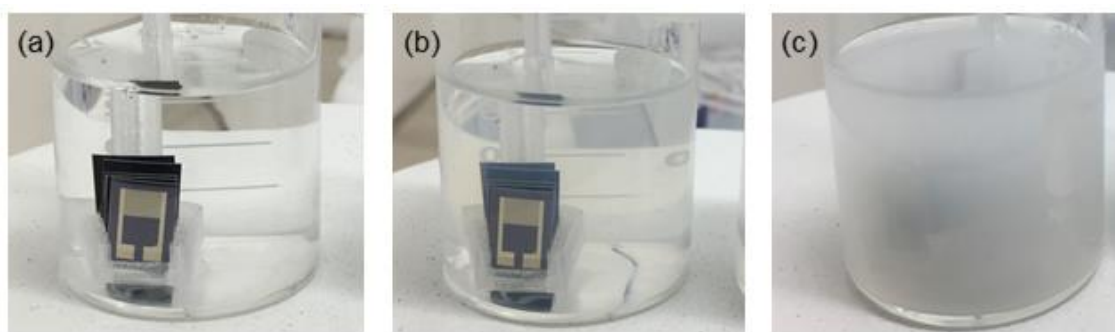
Figure S4: Deposition process for ZIF-8 films: (a) as-deposited, (b) after 10 min, and (c) after 6 h of deposition. For each deposition, five cleaned IDEs were placed in a 3D printed support and immersed into a glass beaker containing a fresh mixture of methanolic $Zn(NO_3)_2$ and 2-methylimidazole solution for 6 h. It is possible to observe a change in color solution within time, going from a translucid to a white opaque. During the deposition, the container was sealed to avoid solution evaporation.
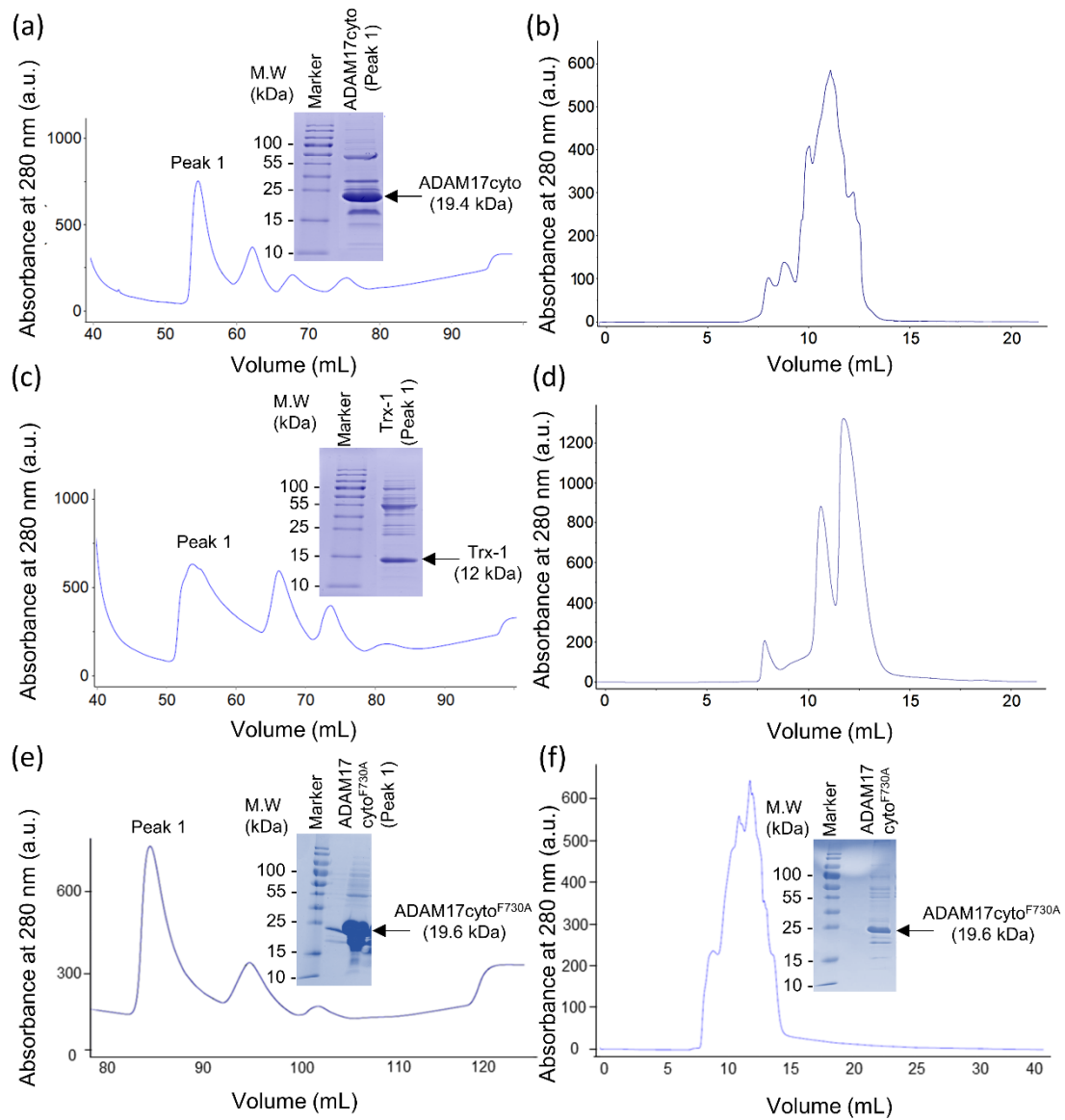
Figure S5: Chromatograms of purified proteins. Recombinant ADAM17cyto protein was expressed in BL21 competent cells and purified through (a) affinity and (b) gel-filtration chromatography. (a) The first peak from ADAM17cyto affinity chromatography was related to the monomeric state of the protein, as observed on the inset of a 15% SDS-PAGE followed by Coomassie blue staining under denaturing conditions. The fractions relative to this first peak were selected to perform gel filtration chromatography. (b) The final purified protein was a mixture of the fractions collected from 10 to 12 mL. Recombinant Trx-1 protein was also purified by (c) affinity and (d) gel-filtration chromatography. (c) The monomeric state of Trx-1 (inset) was observed in the first peak

from affinity chromatography, the fractions relative to this peak were selected to perform gel filtration chromatography. (d) The fractions with higher purity for Trx-1 were collected and combined from 12 to 15 mL. The mutant protein, ADAM17cyto^{F730A}, was purified by (e) affinity and (f) gel-filtration chromatography. (e) The monomeric state of ADAM17cyto^{F730A} (inset) was observed in the first peak from affinity chromatography. (f) The fractions with higher purity for ADAM17cyto^{F730A} were collected and combined, resulting in higher purification, as shown by the inset.
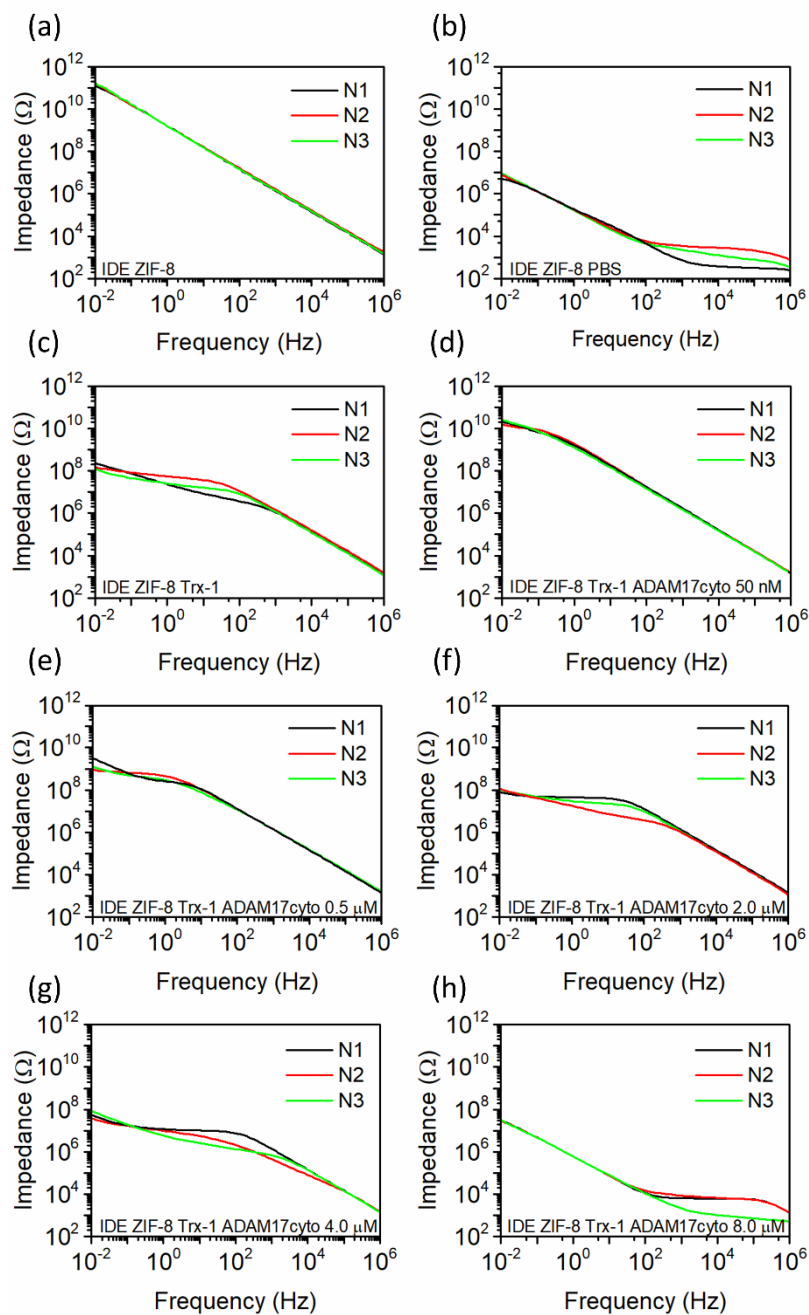
Figure S6: Electrochemical impedance spectroscopy of the modified IDEs. Bode plot analysis shows differences in electrochemical impedance from (a) IDEZ, (b) IDEZ in the presence of PBS, and (c) IDEZT, with Trx-1. It also shows the variance in impedance upon addition of (d) 50 nM, (e) 0.5 µM, (f) 2.0 µM, (g) 4.0 µM, and (h) 8.0 µM of ADAM17cyto purified protein. Measurements were performed in three independent experiments, showing good reproducibility of the developed biosensor.
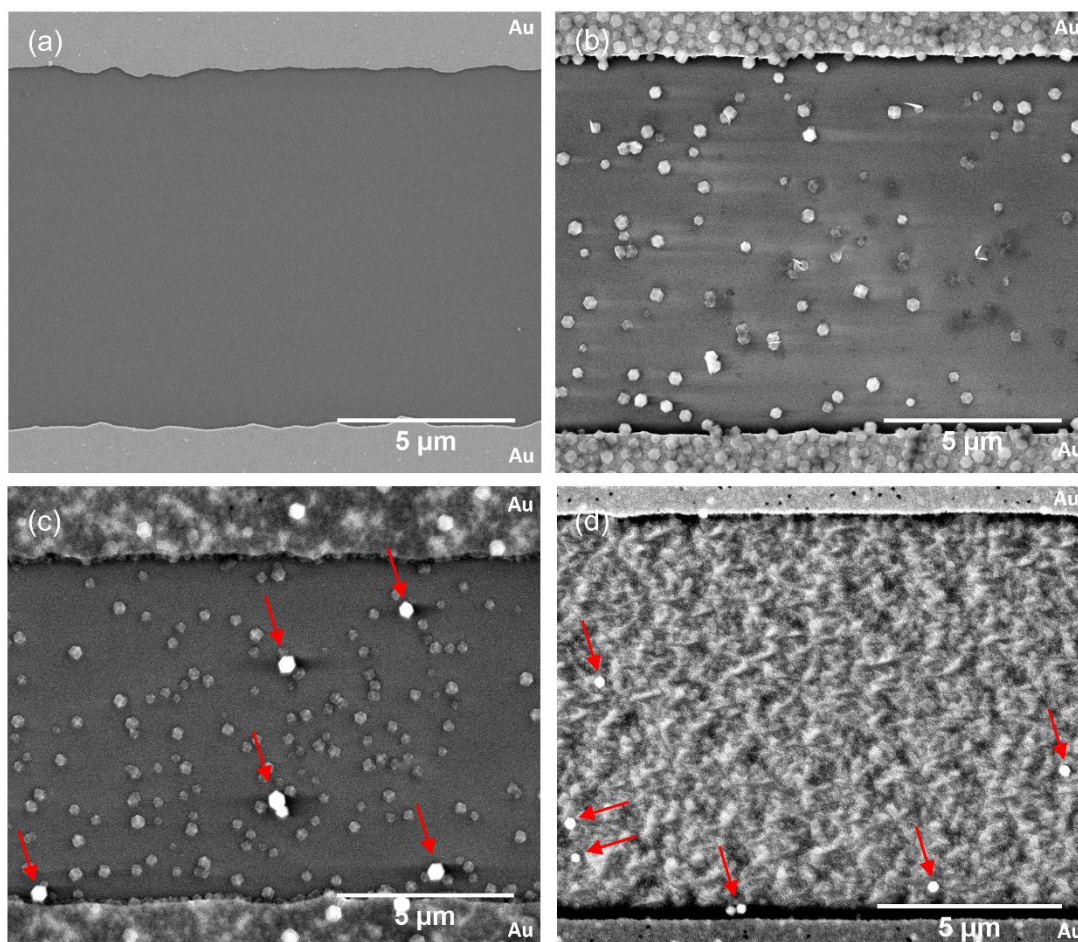
Figure S7: (a) Deposition of ZIF-8 film in function of time. Pristine interdigitated electrode, showing the distance of 10 µm between two Au arrays. After 2 h (b) and 4 h (c) of deposition, it is possible to observe the presence of ZIF-8 particles in the active area, however, it is not enough time to connect the Au arrays. (d) The film formation is only achieved after 6 hours of ZIF-8 deposition, on which it is possible to observe the ZIF-8 particles connecting the Au arrays. Two distinct particle sizes can be identified after 4 h of ZIF-8 deposition, higher particles with 300 ($\pm$ 30) nm are indicated by the red arrows at (c) and (d).
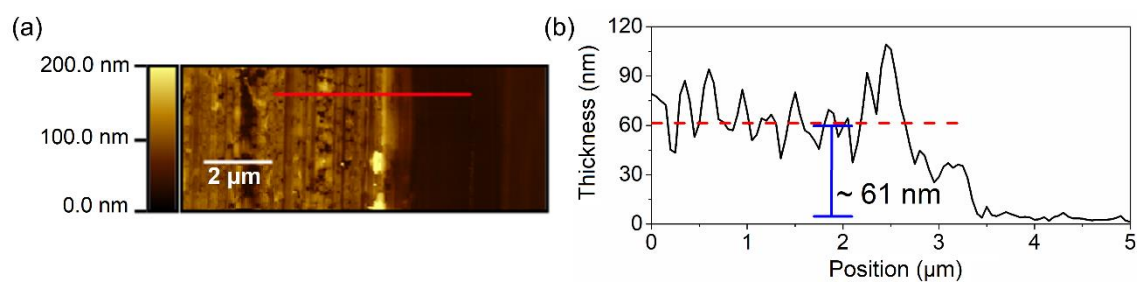
Figure S8: AFM thickness profile of a ZIF8-IDE section. (a) Thickness profile measurement was obtained from the AFM image. (b) The ZIF-8 film presented a thickness of around 61 ($\pm$ 6) nm.
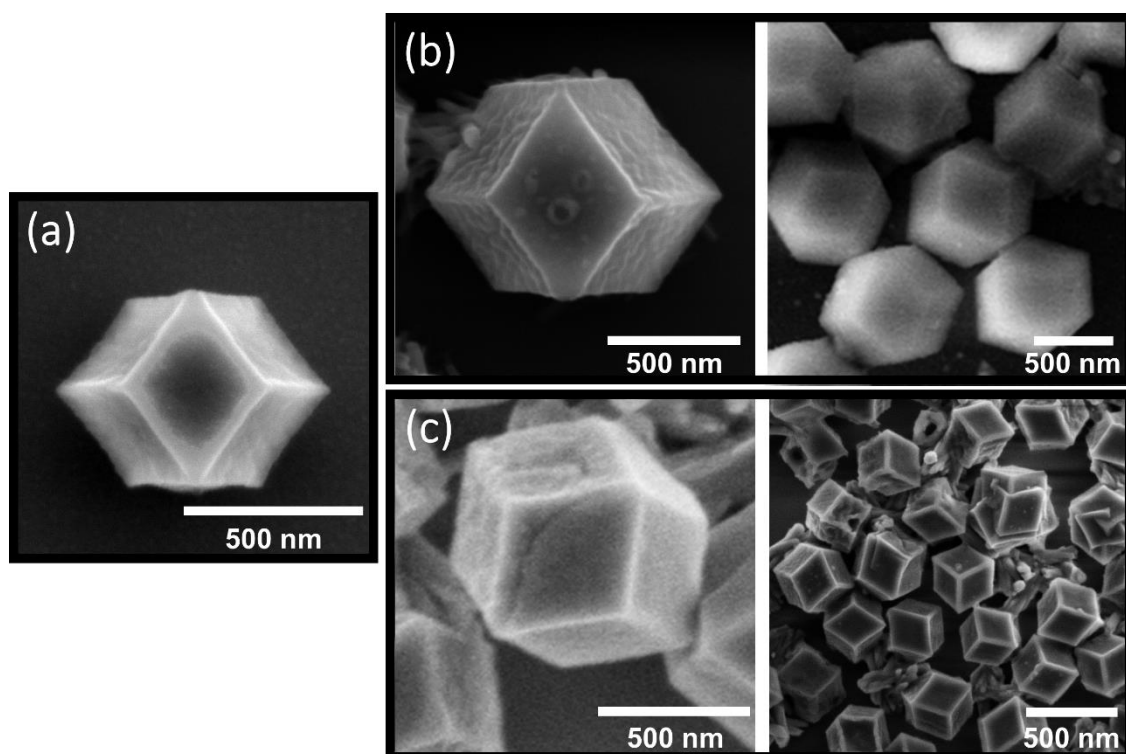
Figure S9: SEM images of ZIF-8 nanoparticles before immersion in PBS solution (a) and after 30 min (b) and 60 min (c) of contact with this buffer. Although some degradation sub-product particles are observed, most of the ZIF-8 nanoparticles did not suffer substantially from etching, showing the same rhombic dodecahedron morphology.
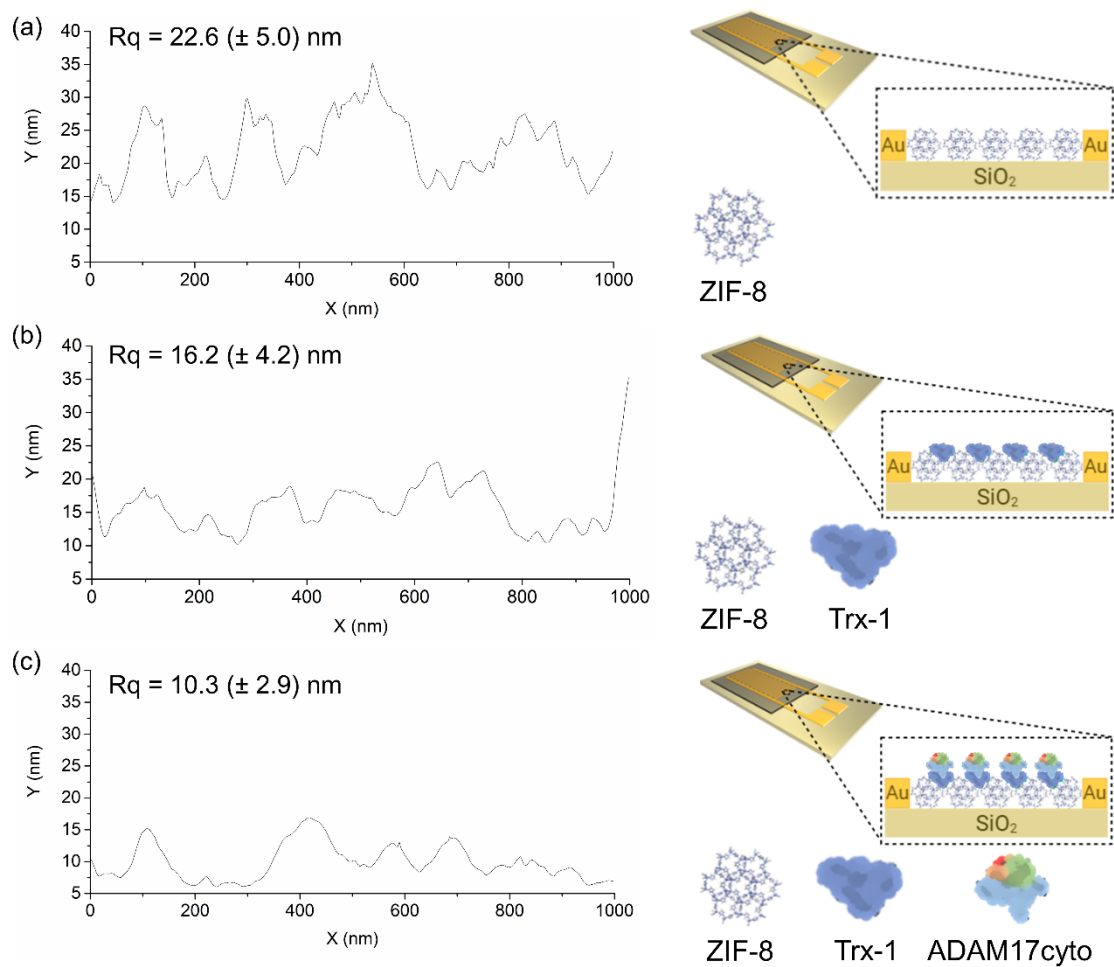
Figure S10: AFM root mean square roughness (Rq) profiles show a decrease in Rq value for IDE modified with ZIF-8 (a) after the incubation with the proteins Trx-1 (b) and ADAM17cyto (c), indicating a homogeneous surface on the IDE active area. The experiment was performed following the described deposition protocol and the ADAM17cyto concentration was 4.0 µM.
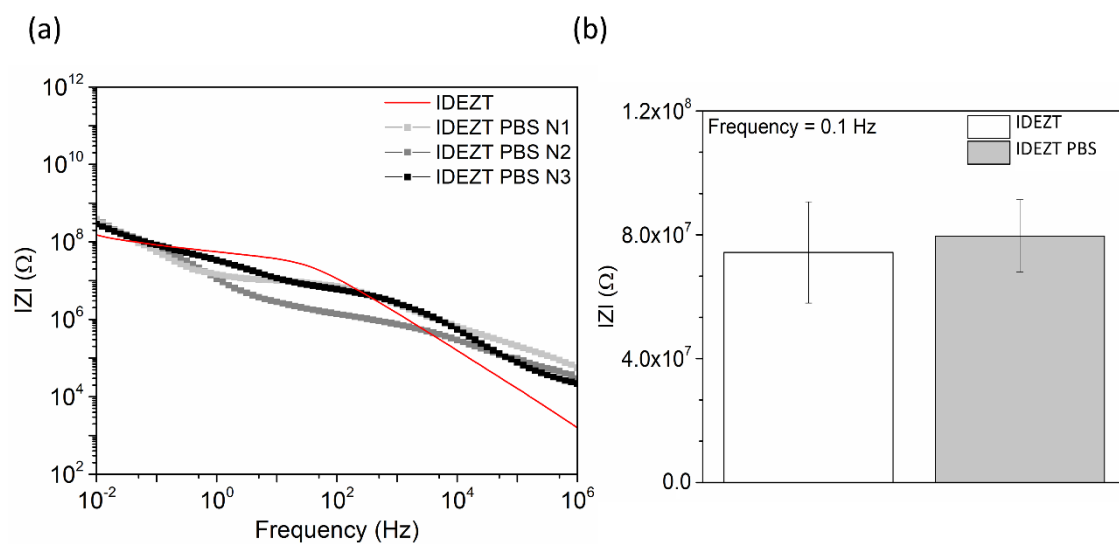
Figure S11: (a) Bode plot from IDEs modified with ZIF-8 and Trx-1 (IDEZT sample), and IDEs modified with ZIF-8 and Trx-1 after 30 min in PBS solution (IDEZT PBS samples), the experiment was performed in three technical replicates. (b) The similar values of impedance between IDEZT and IDEZT PBS samples after PBS immersion indicate a stable interaction between ZIF-8 nanoparticles and Trx-1.
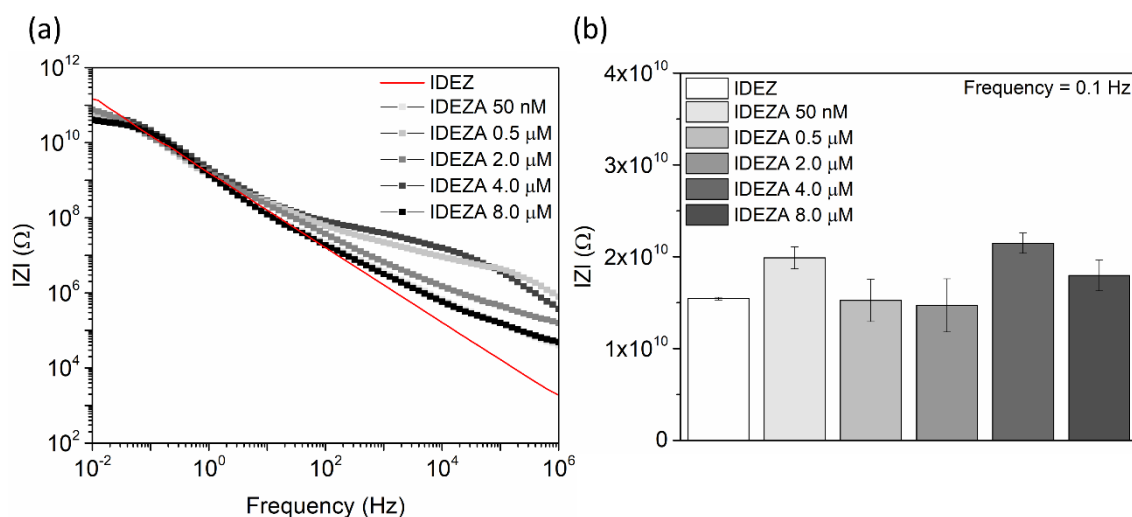
Figure S12: (a) Bode plot from ADAM17cyto directly immobilized on ZIF-8 nanoparticles (IDEZA samples), without Trx-1. (b) Concentrations from 50 nM to 8 µM were immobilized and indicated no significant difference in impedance at 0.1 Hz, when compared to IDEZ. This result shows that no specific and stable interaction between ZIF-8 nanoparticles and ADAM17cyto occur, keeping the impedance in the same range as before ADAM17cyto immobilization. The experiment was performed in three technical replicates.
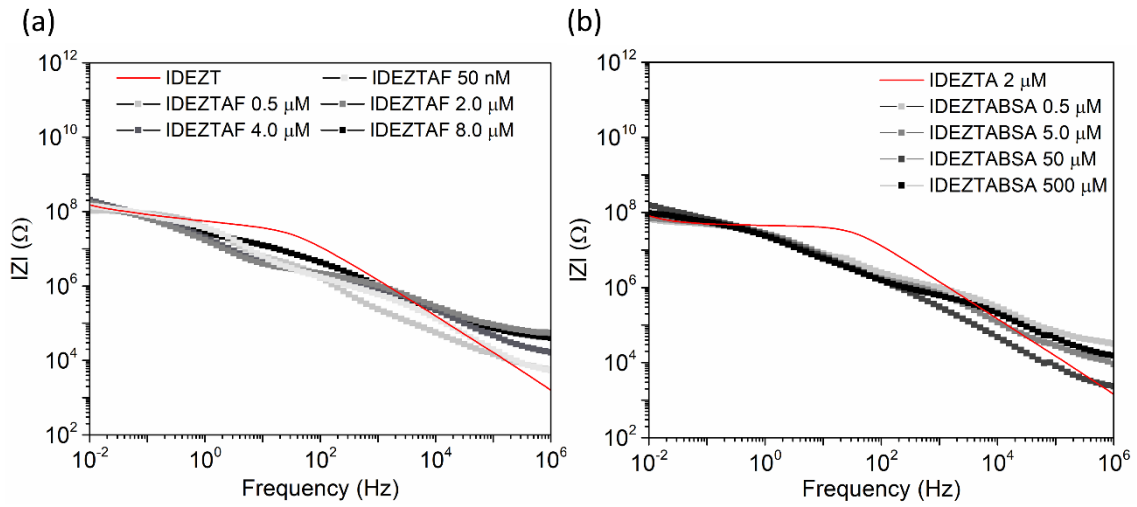
Figure S13: Selectivity evaluation of the ZIF-8 biosensor. (a) A negative control to test false positive detection was performed using ADAM17cyto[F730A] protein, IDEZTAF samples, on which the Bode plot indicates that after exposure to ADAM17cyto[F730A] in different concentrations the impedance at 0.1 Hz remains like IDEZT. (b) The biosensor specificity, using BSA as interfering substance, shows that the impedance is stable and the detection of ADAM17cyto was possible even in concentrations of BSA 250-fold higher than the analyte (IDEZTABSA samples). The experiments were performed in three technical replicates.
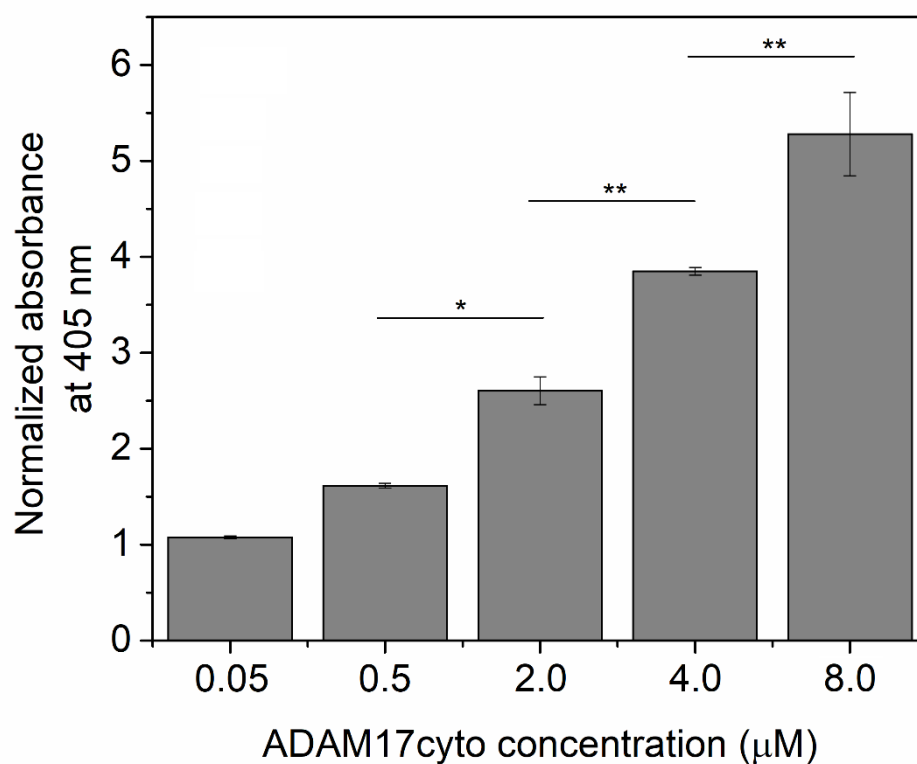
Figure S14: Trx-1 and ADAM17cyto interaction detected by SPB assay with the same concentrations of ADAM17cyto used in the developed biosensor. Statistical analysis was performed by one-way ANOVA and Tukey´s post-test, where $p < 0.05$ was considered to be significant in a 95% confidence interval, P summary; *** = $p < 0.0001$; ** = $p < 0.01$; * = $p < 0.05$ (n=3).